A.2.4 (Much) Wider bandwidths

Wider bandwidth at the telescopes is one the most important goals to be accomplished by the EVN. It will provide both higher sensitivity and increased frequency coverage. Ideally all EVN telescopes would be equipped with low system temperature receivers between 1.4 GHz and 24 GHz; their number should be as low as possible to reduce maintenance efforts and minimise the space needed in the receiver cabins.

Spectral studies

Ultra-wideband receivers will revolutionise our ability to carry out spectral imaging, since it will become possible to obtain information about the intensity of the radio emission at all the frequencies covered by the full bandwidth simultaneously. This will not only be much more efficient and reliable than the earlier practice of combining a few narrow bands, but it will provide much more complete information about the spectra measured, thereby providing much more complete and reliable information about the emission and absorption mechanisms operating in a given region and the corresponding conditions in the radio source. The continuous frequency coverage will enable the identification of particular features in radio spectra and trends displayed by the curvature of the spectrum, rather than just a crude description using a spectral index derived between two fairly widely spaced frequencies.

Polarisation studies - Faraday Rotation mapping

The frequency dependence of the degree of polarisation and the polarisation angle carries a wealth of information about the conditions in the radio source and in its immediate vicinity. Faraday rotation of the linearly polarised waves – as they travel through an ionised medium – is a unique source of information about the magnetic fields and electron densities in thermal plasma in the immediate vicinity of the radio emitting regions. Ultra-wideband receivers will make EVN Faraday rotation studies possible with much more complete and extensive frequency coverage than can be currently carried out with any VLBI system. The technique of "Faraday RM synthesis" will allow us to separate inhomogeneities within the source and along the line of sight, that independently contribute to the Faraday rotation observed. This will have a major impact to the science cases described later in the document.

Possible realisation of ultra-wide bands

For geodetic VLBI, which needs wide instantaneous bandwidths to determine the group delay, a system has been developed that samples 4×1 GHz bands within a range of 2–14 GHz. The EHT currently operates at high frequencies producing a full 64 Gbps per telescope. The technology for wide bandwidth observing clearly is available right now.

The EVN BRAND project aims to develop and build a prototype broad-band digital receiver, with a frequency range from 1.5 GHz to 15.5 GHz, covering the C, M and X band, and opening up new unexplored bands.

Ultra-wide frequency coverage brings with it a set of problems that will need to be tackled. For example disk space availability, lower feed efficiency, correlation capacity, higher connectivity demands and saturation due to RFI. On the other hand, the greatly increased correlated bandwidth will compensate for the lower efficiency, while also providing the option to observe at several widely spaced frequencies. Cost for maintenance and energy for cooling will also be reduced by replacing multiple narrow-band receivers with one wide-band receiver.

The coverage for frequencies above 22 GHz may also be considered at telescopes with a reasonable aperture efficiency and low atmospheric opacity. As mentioned above there is already a

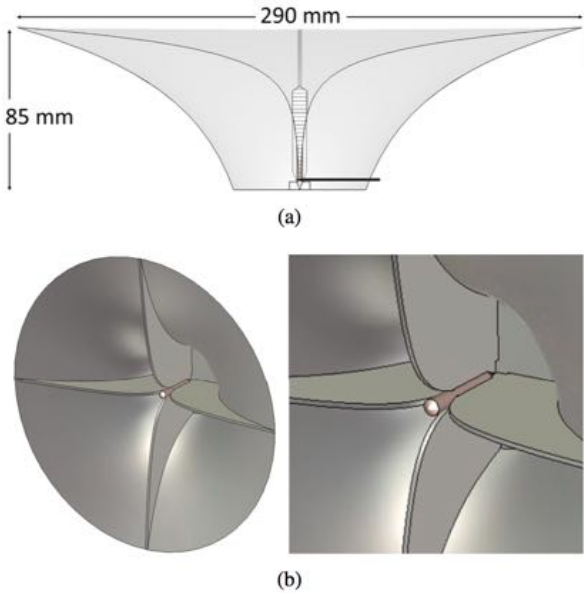

Figure A.2: Feed design for prime focus Effelsberg 100m (Flygare, Pantaleev & Olvhammar 2018). Quad-Ridge Flared Horn (QRFH) illustrated in a) cross-section and b) perspective view with zoom in on the dielectric load at the centre.

de facto standard defined by the KVN which consists of a tri-band receiver simultaneously covering 22, 43 and 86 GHz. The lower frequencies help in determining the noise phase caused by the atmosphere and allow us to increase the integration time at higher frequencies.

Whether the EVN decides to go with a 10:1 system like BRAND, or, like the ngVLA is considering, a suite of wide-band receivers in the 4:1 regime, will no doubt depend on performance, cost and specific science cases. However, it is clear that wide-band observing will be essential for the future of the EVN.

A.2.5 Back-ends: higher rates and flexibility

Future back-ends are likely to be very flexible. There are already some developments towards a 'universal back-end', capable of doing VLBI, continuum, spectral and pulsar observations. These back-ends rely on FPGAs and ADC (Analogue to Digital Converters) with many bits and very high sampling rates. Different observing modes can be implemented by loading different types of firmware. As an example, currently, the Xilinx RFSoC provides an FPGA that includes 8 ADCs with 12 bits and 4 Gsamples per second.

This 'universal back-end' allows for the implementation of algorithms, like band separation, removal of RFI, conversion of linear to circular polarisation (although this can be done off-line as well), packaging and sampling of data into VDIF packets. VDIF packets can be stored for later processing or processed on the fly by other equipment connected via Ethernet.

Alternatively, one could try to separate the sampling from the rest of the processing, sample as much RF or IF as possible and, possibly after coarse channelisation and the distribution of the data stream to several computers, package the sampled data into VDIF packets. A fast ethernet switch would then connect the VDIF output streams to storage, or directly to various CPU/GPU clusters

for different types of processing. In this way VLBI would simply become one of several modes of observing that one could switch to in a matter of minutes.

A.2.6 Radio Frequency Interference

Radio Frequency Interference (RFI) is a severe global problem which will worsen in the future and which will require action from the EVN to mitigate its effects. Its impact on astronomical observations is a major concern for all observatories and may jeopardise the investments to achieve better sensitivity and wider frequency coverage. The RFI from space satellite services has become one of the most severe threats (e.g. Iridium) and requires an urgent global and coordinated response from the radio astronomy community. The plans of SpaceX on the deployment of a constellation of 42000 satellites orbiting the Earth[2] and the first launch of 60 satellites of the *Starlink* constellation in May 2019 highlights such urgency. Around 2000 more satellites are expected in the next 7 years and, according to the documentation sent to the US Federal Communications Commission, they will use nine frequency bands between 10 and 30 GHz jeopardising the usage of wide-band receivers compatible with SKA band 5 and higher frequencies.

Several strategies can be pursued to overcome the effects of RFI:

- Continuous monitoring at the EVN stations. Small antennas covering the frequency interval between 1 and 18 GHz and capable of moving in azimuth and elevation would be a necessary investment to identify the source and frequency of the RFI.
- The installation of High Temperature Superconductor filters prior to the cryogenic LNAs to avoid the saturation of wide band amplifiers.
- An increase of the number of bits to digitise the recorded signal to avoid saturation. Traditionally VLBI has used 2 bits but the presence of strong RFI signals advises the usage of 8 or 10 bits.
- Legal measurements to prohibit the usage of the electromagnetic spectrum in the vicinity of the observatories.
- A global policy defended by the CRAF.
- RFI flagging prior to correlation using advanced algorithms.

A.2.7 Scheduling, monitoring and the Field System

VLBI depends to a high degree on the seamless interaction of many elements, spread around the globe. To make this technique possible at all, many specialised tools and methods have been developed over the years. While still functional, some of these tools are outdated, out of support and consequently very hard to upgrade to the new instruments and observational modes that are constantly being developed.

SCHED is the scheduling programme used by the EVN and several other VLBI networks. It was written entirely in Fortran, in the eighties. Although well written, structured and maintained, the person responsible for its maintenance has recently retired. Both the fact that Fortran as a language is not suited for this type of functionality, and that very few software engineers nowadays are comfortable programming in Fortran, make keeping SCHED up-to-date increasingly problematic.

To address this, a re-factoring of the SCHED software has started. In the new version, named pySCHED, all the existing functionality can still be accessed, albeit through a Python interface, while new functionality, written in Python, can be easily added. Some fairly essential new features have

[2] `https://mc03.manuscriptcentral.com/csb?URL_MASK=5159d9cca5bb40a99ad8bc1739cb141e`, `http://licensing.fcc.gov/myibfs/download.do?attachment_key=1158350`

already been implemented, such as "VEX"2 support and the basic scheduling of DBBC recording. While still at an early stage, this development, making use of a language that has become the de facto standard for scientific programming, should ensure that VLBI scheduling will be able to keep up with future developments.

Although the advent of real-time VLBI has made it far easier to detect problems both at the stations and at the correlator, in a timely fashion, recorded VLBI is still very much needed for many observations. Consequently, monitoring of the network and all its elements remains a crucial part of VLBI observations.

As many VLBI networks are heterogeneous arrays, consisting of widely different telescopes and telescope control systems, designing one single monitoring system is not a trivial task, and more so if this monitoring is coupled to remote control, like in the case of some geodetic stations. Nevertheless, over the years quite a few different monitoring systems have been designed and deployed.

An effort is underway to produce a central, web-based monitoring system, usable for both astronomical and geodetic VLBI. As a first step, an extensive evaluation and rating has been undertaken of the currently existing monitoring systems, their suitability, ease of use, etc. Based on this evaluation a system is being designed that takes advantage of existing monitoring systems at various telescopes and is capable of accessing local databases. This will be followed by the actual integration of existing software into a central infrastructure. The end product should greatly enhance the ability to monitor the performance of the network, and with it, the quality of its data product.

The Field System (FS) is a key element at most VLBI telescopes, controlling the telescope itself, the backend and the recording system. As is the case for SCHED, it is legacy code, written in Fortran and C and developed more than 30 years ago. Its maintenance and development are currently done by NVI Inc, contracted to NASA. Developments are driven by requests from the geodetic and the astronomical communities and some members of these communities actively take part in the debugging of the code. On one specific occasion the EVN has funded the implementation of support for the two main recording modes of the DBBC2.

To ensure its sustainability and prevent a possible fragmentation of the code driven by local needs, the FS could be upgraded and modernised. This should be discussed and agreed upon by NASA, NVI, and technical representatives of the VLBI community as a whole. Modularisation could help to open up the code to contributions from developers from other institutes, and ease the inclusion of different VLBI back-ends. A common basic command syntax for VLBI back-ends and recorders would also greatly facilitate their deployment at different telescopes.

A.2.8 Correlator

Software correlators have seen a tremendous development over the past decade. The JIVE-developed SFXC has gone from first fringes in 2007 to becoming a powerful, highly versatile, flexible and multi-functional backbone of the EVN network. Moore's law has easily kept up with increasing bit rates, and to this date (2020) the correlator capacity has never been a bottleneck in EVN operations.

Over the years, other solutions have been considered and developed, mainly driven by the assumption that data rates would grow at such a rate that CPU-based software correlators would quickly be overwhelmed, an assumption that did not materialise. However, with the advent of ultra-wide-band receivers this issue may have to be reconsidered.

One of these solutions was the JUC, the JIVE UniBoard Correlator, a Field Programmable Gate Array (FPGA)-based computing platform. Although powerful and energy-efficient, such platforms tend to take a very long time to develop and debug, while the implementation of firmware

modifications equally is a very lengthy process. Simply put, they are highly suitable for the processing of large identical data streams, with identical data formats and rates. Many VLBI arrays are by their very nature inhomogeneous, deploying different equipment which moreover is constantly being upgraded. This, combined with their lack of flexibility, severely limits the usefulness of FPGAs in VLBI correlation.

Correlation on Graphics Processing Units (GPU) has been successfully implemented, an example being the LOFAR COBALT correlator. For VLBI arrays however, consisting of relatively few array elements (10 to 30 telescopes), GPUs do not seem to bring a substantial improvement. In 2018, during a hackathon in Perth, engineers from CSIRO, Swinburne and JIVE collaborated to port parts of the DIFX software correlator to a GPU platform, aided by a number of GPU experts. The final result was that the gain in correlation speed compared to a CPU of similar price, was roughly a factor of two. The main bottleneck for VLBI correlation seems to be the memory access between GPU and its memory, causing only 10 to 20% of compute resources to be actually used. It should be noted that GPUs are in constant development, and new versions may be better suited to the VLBI use case. A hybrid approach using both CPUs and GPUs may be the way of the future; it might be possible to run large-bandwidth continuum correlation on GPUs while reserving the more flexible CPUs for non-standard, complex and/or innovative correlation jobs.

Cloud correlation has finally been suggested as a solution to cope with the large data streams that geodetical and astronomical VLBI are, or will start, producing in the near future. Recently, this has been investigated by Gill et al. (2019). In this case, too, a hybrid approach may be optimal, for example by using HPC/cloud resources for occasional high-volume standard correlation jobs and an in-house correlator for experimental work. Whether such a solution will ever be economically/logistically feasible is not entirely clear, but it is certainly worth investigating in the coming years.

A.2.9 Future improvements

In the following section, we list the improvements that are technically feasible on time scales of 5 and 10 years.

Five years

- Wide-band receivers on at least a sub-set of the EVN. What frequency range will be covered is unclear, and will no doubt partly depend on the performance and cost of BRAND, partly on specific science cases. Aiming for maximum sensitivity by using the full band will of course bring its own set of problems, in terms of availability of media, connectivity, correlation capacity. However, there will be fewer receivers to maintain, and multiple discontinuous bands can be observed simultaneously.
- At higher frequencies, multi-band receivers like the KVN quasi-optics system on a sub-set of the EVN. These are large systems that are not suitable for prime focus, but a compact prototype has been developed recently (Han et al. 2017).
- DBBC3 backends at all stations.
- RFI mitigation at the stations (in-built feature of DBBC3).
- Multiple 100G connectivity to JIVE.
- Inclusion of Quasar VLBI Network telescopes in real-time operations.
- Inclusion of Ghana, Xi'An, MeerKAT telescopes.
- Regular correlation of geodetic observations at JIVE.
- (semi-) Automated follow-up of transient events by sub-set of EVN stations.

- EVN-light observations, e.g. more regular observing sessions within a subset of EVN stations.
- Upgraded scheduling and common monitoring tools.

Ten years

- 'Real' global VLBI, seamless cooperation of different networks.
- Global VLBI with the SKA.
- Deployment of 'Software Defined Radio' back-ends, to some degree doing away with the need for different hardware back-ends for VLBI, pulsar astronomy, etc. Such a system would isolate the digitisation step from the rest of the back-end, sampling the RF signal, or IF, and packaging the samples into VDIF packets. These VDIF packets can be stored for later processing or processed on the fly by any suitable piece of equipment, connected via Ethernet. Such a system is currently being considered at the VLBA.
- True wide-field VLBI, enabling high-resolution blind surveys.
- Upgraded software control tools for telescopes and backends.

A.3 Spectral lines of interest to radio astronomy (∼<100 GHz)

Atom/molecule	Line name	Rest frequency [GHz]
H I	neutral hydrogen	1.420405752
OH	hydroxyl radical	1.6122310
OH	hydroxyl radical	1.6654018
OH	hydroxyl radical	1.6673590
OH	hydroxyl radical	1.7205300
CH	methylidyne	3.263794
CH	methylidyne	3.335481
CH	methylidyne	3.349193
OH	hydroxyl radical	4.660242
OH	hydroxyl radical	4.765562
H_2CO	ortho-formaldehyde	4.829660
OH	hydroxyl radical	6.030747
OH	hydroxyl radical	6.035092
CH_3OH	methanol	6.668518
HC_3N	cyanoacetylene	9.098332
CH_3OH	methanol	9.936202
CH_3OH	methanol	12.178593
OH	hydroxyl radical	13.4414173
H_2CO	ortho-formaldehyde	14.488490
C_3H_2	ortho-cyclopropenylidene	18.343145
NH_3	para-ammonia	18.499390
NH_3	ortho-ammonia	19.757538
CH_3OH	methanol	19.967415
NH_3	para-ammonia	20.804830
NH_3	ortho-ammonia	21.070739
H_2O	ortho-water	22.23507985
NH_3	para-ammonia	22.653022
CH_3OH	methanol	23.121024
NH_3	para-ammonia	23.694506
NH_3	para-ammonia	23.722634
NH_3	ortho-ammonia	23.870130
CH_3OH	methanol	24.9287
CH_3OH	methanol	24.933468
CH_3OH	methanol	24.95908
CH_3OH	methanol	25.018123
NH_3	ortho-ammonia	25.056025

With help from Katharina Immer. Useful resources: `https://www.narrabri.atnf.csiro.au/observing/spectral.html` compiled by Bob Sault and Robin Wark. Also see Lovas, Snyder & Johnson "Recommended rest frequencies for observed interstellar molecular transitions" (1979), Wilson, Rohlfs, & Hüttemeister "Tools of radio astronomy" (1986), and Malcolm Gray "Maser sources in astrophysics" (2012). More molecules/transitions are available in the Lovas search engine: `https://physics.nist.gov/cgi-bin/micro/table5/start.pl`

Atom/molecule	Line name	Rest frequency [GHz]
CH_3OH	methanol	25.124873
CH_3OH	methanol	25.294411
CH_3OH	methanol	25.54143
CH_3OH	methanol	25.87818
CH_3OH	methanol	26.84727
CH_3OH	methanol	27.47258
CH_3OH	methanol	28.16952
CH_3OH	methanol	28.90585
CH_3OH	methanol	28.9699
CH_3OH	methanol	29.63711
CH_3OH	methanol	30.30808
NH_3	ortho-ammonia	31.424943
CH_3OH	methanol	36.16924
CH_3OH	methanol	37.70372
CH_3OH	methanol	38.2935
CH_3OH	methanol	38.4526
SiO	silicon monoxide	42.820570
SiO	silicon monoxide	43.122090
SiO	silicon monoxide	43.423853
CH_3OH	methanol	44.06949
CS	carbon monosulfide	48.990955
DCO^+	deuterated formylium	72.039331
DCN	deuterated hydrogen cyanide	72.413484
CH_3OH	methanol	84.521169
SiO	silicon monoxide	85.640456
SiO	silicon monoxide	86.243442
CH_3OH	methanol	86.615602
$H^{13}CO^+$	formylium	86.754294
SiO	silicon monoxide	86.846998
CH_3OH	methanol	86.9029479
HCN	hydrogen cyanide	88.631847
HCO^+	formylium	89.188518
HNC	hydrogen isocyanide	90.663574
N_2H^+	diazenylium	93.173809
CH_3OH	methanol	95.16944
H_2O	para-water	96.26116
CS	carbon monosulfide	97.980968
CH_3OH	methanol	107.01385
CH_3OH	methanol	108.893963
$C^{18}O$	carbon monoxide	109.782182
^{13}CO	carbon monoxide	110.20137
CO *	carbon monoxide	115.271203

* redshifted CO for $z > 1.67$ falls in the Q-band (43 GHz).

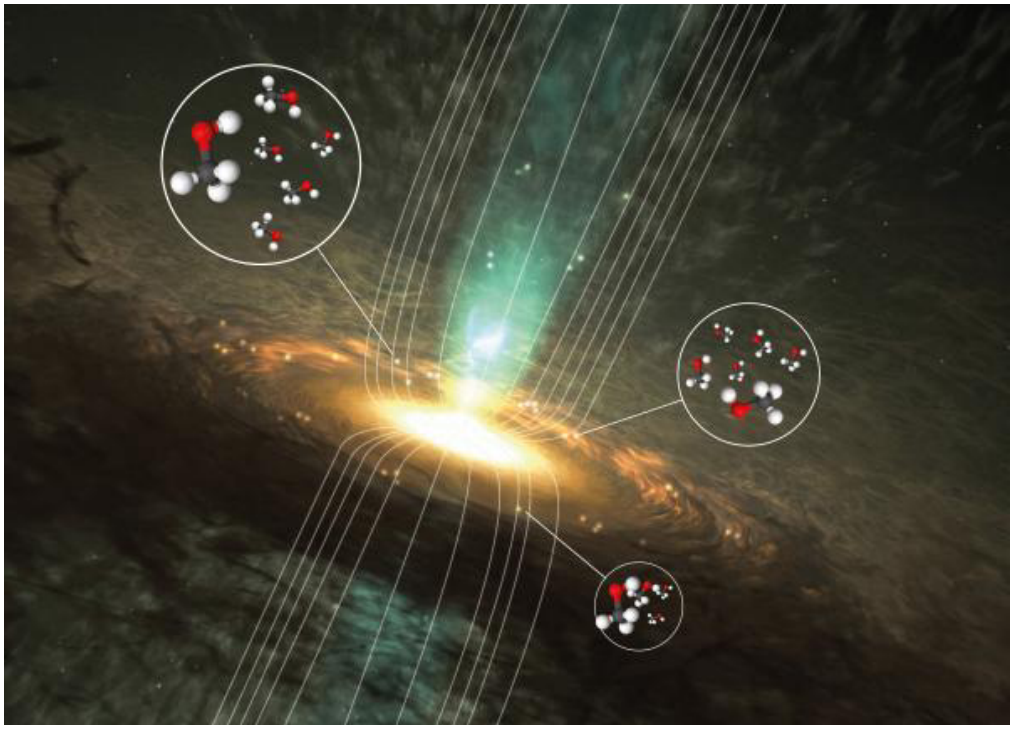

Figure A.3: Magnetic fields play an important role in the places where most massive stars are born. This illustration shows the surroundings of a forming massive star, and the bright regions where radio signals from methanol can be found. The bright spots represent methanol masers - natural lasers that are common in the dense environments where massive stars form - and the curved lines represent the magnetic field. Thanks to new calculations by astrochemists, astronomers can now start to investigate magnetic fields in space by measuring the radio signals from methanol molecules in these bright sources. (JIVE press release: `http://www.jive.eu/astrochemists-reveal-magnetic-secrets-methanol`) Credit: Wolfgang Steffen/Chalmers/Boy Lankhaar (molecules: Wikimedia Commons/Ben Mills).

REFERENCES

Abbott, B.P. et al., 2017, *ApJ*, **848**, L12
Abramowski, A. et al., 2012, *ApJ*, **746**, 151
Acciari, V. A. et al., 2009, *Science*, **325**, 444
Ackermann, M. et al., 2016, *ApJS*, **222**, 5
Akiyama, K. et al., 2016, *ApJL*, **823**, L26
Aleksić, J. et al., 2014, *Science*, **346**, 1080
Alexander, K.D. et al., 2017, *ApJL*, **848**, L21
An, T. et al., 2012, *ApJS*, **198**, 5
An, T., Sohn, B.W., & Imai, H., 2018, *Nature Astron.*, **2**, 118
Ansoldi, S. et al., 2018, *ApJL*, **863**, L10
Bansal, K. et al., 2017, *ApJ*, **843**, 14
Beswick, R. J. et al., 2015, *PoS["AASKA14"]1041*
Buch, K. D. et al., 2017, *Jl. Astron. Instru.*, in press [arXiv:1710.08576]
Callingham, J. R. et al., 2017, *ApJ*, **836**, 174
Chandra, P. et al., 2016, *Jl. Astron. Instru.*, 37, 30
Chatterjee, S. et al., 2017, *Nature*, **541**, 58
Clarke, T. E. et al., 2016 [arXiv:1603.03080]
Deller, A.T. et al., 2007, *PASP*, **119**, 318
Deller, A.T. et al., 2011, *PASP*, **123**, 275
Ellingson, S. W. et al., 2013, *IEEE Trans. on Antennas & Propagation*
Flygare, J., Pantaleev, M. & Olvhammar, S., 2018, *Proc. EuCAP 2018* [online]
Ghirlanda, G. et al., 2019, *Science*, **363**, 968 [arXiv:1808.00469]
Gill, A. et al., 2019, *PASP*, 131, 4501 Giroletti, M. et al., 2012, *A&A*, **538**, L10
Goddi, C. et al., 2019, *PASP*, **131**, 075003
Gupta, Y. et al., 2017, *Current Science*, **60**, 95
Gurvits, L. et al., 2019, ESA Voyage 2050 White Paper [arXiv:1908.10767]
Gurvits, L.I., 2020a, *Advances in Space Research*, **65(2)**, 703
Gurvits, L.I., 2020b, *Advances in Space Research*, **65(2)**, 868
Han, S.-T. et al., 2017, *J. Infrared, Millimeter, & Terahertz Waves*, **38(12)**, 1487
Heywood, I. et al., 2011 [arXiv:1103.1214]
IceCube Collaboration et al., 2018, *Science*, **361**, 1378
Intema, H. T. et al., 2017, *A&A*, **598**, A78
Ishwara-Chandra, C. H., 2010, *MNRAS*, **405**, 436
Issaoun, S., et al., 2019, *ApJ*, **871**, 30
Kale, R. et al., *Jl. Astrophys. Astr.*, **37**, 31
Kanekar, N., 2014, *ApJL*, **797**, L20
Keimpema, A. et al., 2015, *Experimental Astronomy*, **39**, 259
Kettenis, M. et al., 2006, *ASP COnf. Ser.*, **351**, 497
Kharb, P. et al., *Jl. Astrophys. Astr.*, **37**, 34
Kim, J.-Y. et al., 2018, *A&A*, **616**, A188
Kloeckner, H.-R. et al., 2011 [arXiv:1103.3600]
Krishnan, V. et al., 2017, *MNRAS*, **465**, 1095
Kun, E., Biermann P.L., & Gergely L.Á., 2019, *MNRAS*, **483**, L42
Lacy, M. et al. 2019 [arXiv:1907.01981]

Law, C.J. et al., 2018, *ApJS*, **236**, 8
Li, Z. et al., 2018, *MNRAS*, **476**, 399
Lico, R. et al., 2017, *A&A*, **606**, A138
Lovas, F.J., Johnson, D.R., & Snyder, L.E., 1979, *ApJS*, **41**, 451
Marcote, B. et al., 2017, *ApJL*, **834**, L8
Matthews, L.D. et al., 2018, *PASP*, **130**, 015002
Mattila, S. et al. 2018, *Science*, **361**, 482
Miller-Jones, J.C.A. et al., 2018, *MNRAS*, **479**, 4849
Mooley, K.P. et al., 2018, *Nature*, **561**, 355
Moscadelli, L. et al., 2019, *A&A*, **622**, A206
Nan, R., & Zhang, H., 2017, *Nature*, **1**, 12
Napier, P.J. et al., 1994, *Proc. IEEE*, **82**, 658
Prandoni, I. & Seymour, N., 2015, *PoS["AASKA14"]991*
Reid, M.J. et al., 2014, *ApJ*, **783**, 130
Reynolds, C., Paragi, Z., & Garrett, M., 2002 [arXiv:astro-ph/0205118]
Roy, S. et al., 2010, *ApJL*, **712**, L5
Sanna, A. et al., 2017, *Science*, **358**, 227
Schilizzi, R.T., 1995, *ASP Conf. Ser.*, **82**, 397
Shu, F. et al., 2017, *ApJS*, **230**, 13
Straal, S.M. et al., 2016, *ApJ*, **822**, 117
Swarup, G. et al., *Current Science*, **60**, 95
Szomoru, A., 2008, *PoS["IX EVN Symposium"]40*
Taylor, G.B. et al., 2012, *Journal of Astronomical Instrumentation*, **1**, 1250004
The Event Horizon Telescope Collaboration, et al., 2019a *ApJL*, **875**, L1
The Event Horizon Telescope Collaboration, et al., 2019b *ApJL*, **875**, L2
The Event Horizon Telescope Collaboration, et al., 2019c *ApJL*, **875**, L3
The Event Horizon Telescope Collaboration, et al., 2019d *ApJL*, **875**, L4
The Event Horizon Telescope Collaboration, et al., 2019e *ApJL*, **875**, L5
The Event Horizon Telescope Collaboration, et al., 2019f *ApJL*, **875**, L6
Tingay, S. et al., 2013, *PASA*, **30**, 7
Tong, F., Zheng, W., & Shu, F., 2014, *Chinese Science Bulletin*, **59**, 3362
Ye, S., Wan, T., & Qian, Z., 1991, *IAU Colloq.*, **131**, 386
Zensus, J.A., Ros, E., 2015 [arXiv:1501.05079]
van Haarlem, M.P. et al., 2013, *A&A*, **556**, A2

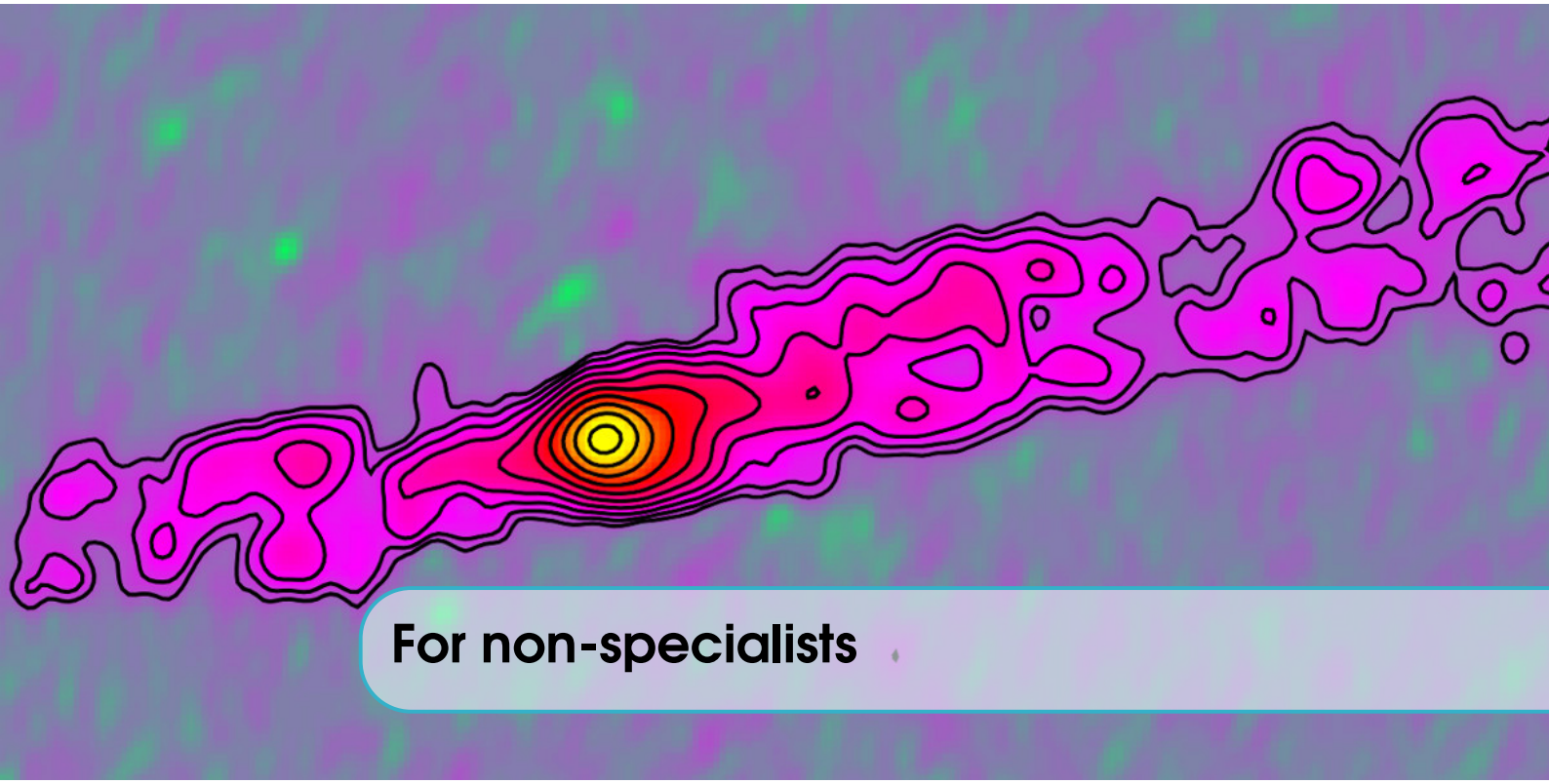

For non-specialists

"VEX" VLBI schedules are written in vex-format files. These are used to control antennas for observations.. 174

***uv*-coordinates** VLBI interferometers sample the data in the *uv*-plane, which is in a Fourier relation with the sky brightness distribution. A higher number of telescopes and longer observing time mean more dense sampling of the acrshortuv-plane, i.e. better *uv*-coverage – also depending on the distribution of the antennas. This results in higher fidelity and more sensitive images of the radio sky. 10

e-EVN Is a subset of the EVN telescopes participating in real-time e-VLBI operations. All telescopes are in principle e-VLBI capable, albeit different data rate limits may apply. 6

e-VLBI Is real-time data transfer and correlation through high-speed networks using a software correlator. The EVN and JIVE have played a pioneering role in the development of the e-VLBI technique. 148

EVN The European VLBI Network is the most sensitive standalone VLBI array to date. It includes some of the greatest radio antennas in Europe, Africa, Asia and the Caribbeans. 3

EVN-light Is a concept of using part of the EVN array for VLBI observations outside of regular disc recording sessions. 15, 170

JIVE The Joint Institute for VLBI ERIC was formerly known as the Joint Institute for VLBI in Europe, and generally referred to as JIVE. It is a European Research Infrastructure Consortium (formally registered as JIV-ERIC) based in Dwingeloo, Netherlands. It operates the central data processor of the EVN. 3

SFXC The EVN software correlator at JIVE. 92

SKA-VLBI Is a concept to include phased-up phase-I. SKA telescopes in VLBI observations. The EVN will have joint sky coverage with SKA1-MID. 141, 152

SKA1-MID Is the planned, phase-I. mid-frequency telescope of the Square Kilometre Array in South Africa. 5

Space VLBI The resolving power of a VLBI array depends on the largest distances between its elements. The longer these 'baselines' are, the finer details the images will have. In space VLBI one (or in the future, possibly more) of the telescopes is in space, to overcome the natural limitation to the maximum baselines a VLBI array can have on Earth.. 15, 167

VLBI Very Long Baseline Interferometry is a technique that combines radio telescopes at great distances, to produce the highest angular resolution images in astronomy. 3

VLBI image of the archetypal radio galaxy Cygnus A at the frequency of 86 GHz. The high spatial resolution gives insight into the transverse width profile at the onset of the two-sided flow. The jet base appears wide with a minimum width of 227 Schwarzschild radius RS. This is significantly larger than the radius of the innermost stable circular orbit (ISCO), suggesting that the emission is produced by a mildly relativistic, parabolically expanding outer disk wind. The existence of a central and faster jet, possibly driven by the rotation of the inner regions of the accretion disk or by the spinning black hole and invisible due to Doppler deboosting, is suggested by the kinematic properties and by the observed limb brightening of the flow. Credit: Boccardi et al. (2016), *A&A*, **588**, L9, reproduced with permission

Acronyms and more...

***e*-MERGE** *e*-MERlin Galaxy Evolution survey. 38, 39

***e*-MERLIN** *enhanced* Multi-Element Remotely Linked Interferometer Network. 5, 7, 11, 15, 37–40, 42, 50, 51, 96, 97, 105, 112–114, 122, 124–126, 140, 141, 148, 157, 168–170

uv *uv*-coordinates/plane/coverage. 10, 25, 26, 46, 52, 61, 70, 72, 78, 82, 91–93, 97, 125–127, 142, 148, 149, 152, 165, 169, 170, 183

Athena Advanced Telescope for High-ENergy Astrophysics. 7

Chandra Chandra X-ray Observatory. 37, 38, 69

Euclid Euclid satellite. 7, 17, 18

Fermi Fermi Gamma-ray Space Telescope. 63, 64, 86, 142, 146

Gaia Gaia mission. 10, 79, 80, 95, 105, 122, 123, 128, 132–134, 142, 152

HALCA Highly Advanced Laboratory for Communication and Astronomy. 167

HST Hubble Space Telescope. 21, 69, 85, 142

IKAROS Interplanetary Kite-craft Accelerated by Radiation Of the Sun. 135

IXPE X-ray Polarimetry Explorer. 78

JUICE Jupiter Icy Satellites Explorer. 136

JWST James Webb Space Telescope. 7, 72, 142

Kepler Kepler Space Telescope. 96

LISA Laser Interferometer Space Antenna. 9, 68, 144, 147, 159

MSX Midcourse Space Experiment. 124

Planck Planck satellite. 17

RadioAstron Space VLBI mission. 58, 59, 136, 155, 167

SELENE Selenological and Engineering Explorer. 135

Spektr-R Space VLBI telescope – *RadioAstron* mission. 167

Starlink Satellite constellation being constructed by American company SpaceX to provide satellite Internet access. 173

Swift Neil Gehrels Swift Observatory; formerly Swift Gamma-Ray Burst Mission. 64, 84, 86, 142

VSOP VLBI Space Observatory Programme. 167

XIPE X-ray Imaging Polarimetry Explorer. 78

eROSITA X-ray instrument on Spektr-RG. 52, 142

ADC Analog-to-digital Converter. 172
AGB Asymptotic Giant Branch. 112, 114, 120, 122–126
AGN Active Galactic Nuclei. 6, 9, 13, 14, 23, 24, 26, 27, 29, 36–40, 43, 44, 46–52, 55–60, 62–76, 78, 85, 92, 104, 131–133, 141, 146, 148, 149, 151, 156, 157
AIPS Astronomical Image Processing System. 126
ALMA Atacama Large Millimeter/submillimeter Array. 7, 15, 51, 52, 103–105, 112–114, 121, 123, 124, 126, 127, 142, 159, 161, 166
APERTIF APERture Tile In Focus. 7, 50, 52, 93, 168
ASASSN All-Sky Automated Survey for Supernovae. 84
ASKAP Australian Square Kilometre Array Pathfinder. 50, 90, 93, 111, 113, 149, 161
ASTRON Netherlands Institute for Radio Astronomy. 11
ATCA Australia Telescope Compact Array. 78, 160, 161
ATNF Australia Telescope National Facility, Marsfield, Australia. 160
AU Astronomical Unit. 98, 104, 113, 116–120, 127, 145
AVN African VLBI Network. 108, 125, 127, 140, 145, 149, 157

BAaDE Bulge Asymmetries and Dynamical Evolution. 123, 124
BAO Baryon Acoustic Oscillation. 18, 20, 26, 29
BAT *Swift* Burst Alert Telescope. 64
BeSSel Bar and Spiral Structure Legacy Survey. 123
BH Black Hole. 71, 77–80, 88, 144, 147, 154
BKG Federal Agency for Cartography and Geodesy, Frankfurt am Main, Germany. 11
BL-Ic Broad-line type Ic supernova. 83, 84
BLR Broad Line Region. 43
BNS Binary Neutron Star. 88
BRAND BRoad bAND EVN. 31, 61, 62, 125, 168, 171, 172, 175

CASA Common Astronomy Software Applications. 126, 150, 151
CBD Consortium Board of Directors. 155, 156
CCSN Core-collapse Supernova. 82
CDM Cold Dark Matter. 17, 19, 23, 66
CH_3OH methanol. 103, 117–119, 151, 177, 178
CHIME Canadian Hydrogen Intensity Mapping Experiment. 7, 90, 93, 142
CLASS Cosmic Lens All-Sky Survey. 21, 22, 24
CMB Cosmic Microwawe Background. 17, 18, 27, 29
CME Coronal Mass Ejection. 108, 109
CO Carbon monixide. 51
COBRaS Cygnus OB2 Radio Survey. 112, 114
COSMOS Cosmic Evolution Survey. 67
CPU Central Processing Unit. 169, 172, 174, 175
CRAF Committee on Radio Astronomical Frequencies. 173
CSE Circumstellar Envelope. 120, 121, 124, 126
CSIRO Commonwealth Scientific and Industrial Research Organisation, Canberra, Australia. 160, 175
CSO Compact Symmetric Object. 66, 151

CTA Cherenkov Telescope Array. 7, 142, 145, 146, 152
CVN Chinese VLBI Network. 15, 158

DBBC Digital Base Band Converter. 161, 168, 174, 175
DeltaDOR Delta-Differential One-Way Ranging. 135
DES Dark Energy Survey. 17
DiFX Distributed FX-style software correlator. 159–161
DM Dispersion Measure. 89
DR2 Gaia Data Release 2. 79
DSA-10 Deep Synoptic Array. 90
DSN Deep Space Network. 135

E-CDFS Extended Chandra Deep Field-South. 36
EAVN East Asian VLBI Network. 15, 62, 139, 158–160
EC-H2020 European Commission Horizon 2020 programme. 3
ECM Electron Cyclotron Maser. 109
EGP Extrasolar Giant Planet. 111
EHT Event Horizon Telescope. 10, 58, 59, 62, 139, 159, 162, 166, 171
ELT Extremely Large Telescope. 7, 94, 142, 144, 145, 152
EM Electromagnetic. 68, 144, 147
EMU Evolutionary Map of the Universe. 113
ERIC European Research Infrastructure Consortium. 156
ERIS European Radio Interferometry School. 140
ESA European Space Agency. 17, 122, 135–137, 144, 152, 180
ESTRACK European Space Tracking. 135
EVN European VLBI Network. 1, 3, 5–8, 10, 14, 15, 17, 19, 20, 25, 26, 31, 38–41, 44, 46, 49–52, 57, 62, 65–67, 69, 71, 72, 77, 81, 82, 84–86, 88, 90, 92–98, 101, 105, 107–110, 113, 114, 117–127, 134–137, 139–142, 144–152, 155–160, 166–176, 181

FAST Five-hundred-meter Aperture Spherical radio Telescope. 93–95, 97, 148, 158, 159, 169, 170
FIRST Faint Images of the Radio Sky at Twenty-Centimeters. 63, 64
FoV Field of View. 90, 92, 93, 96
FPGA Field-programmable Gate Array. 168, 172, 174, 175
FR Fanaroff-Riley. 68
FRB Fast Radio Burst. 89–93, 139, 141, 147, 152, 156, 162
FUV Far ultraviolet light. 36
FWHM Full Width at Half Maximum. 38, 61, 88, 144

GÉANT Pan-European data network for research and education. 168
Gbps Gigabit per second. 10, 95, 148, 160, 161, 168–171
GBT Robert C. Byrd Green Bank Telescope. 17, 20, 97, 161
GLT Greenland Telescope Project. 161
GMRT Giant Metrewave Radio Telescope. 164, 165
GMVA Global Millimeter VLBI Array. 58, 59, 61, 62, 139, 155, 159, 161, 166
GOBELINS Gould's Belt Distances Survey. 106, 107
GOODS-N Great Observatories Origins Deep Survey - North. 38, 147
GPU Graphics Processing Unit. 161, 169, 170, 172, 175

GRB Gamma Ray Burst. 35, 82–84, 86–88, 90
GUT Grand Unified Theory. 147
GW Gravitational Wave. 28, 30, 68, 70, 86, 94, 142, 144, 156, 159, 162

H_2O water. 7, 46, 103, 116, 117, 120, 121, 126, 177, 178
HBA LOFAR High Band Antenna. 163
HDF Hubble Deep Field. 147
HERA Hydrogen Epoch of Reionisation Array. 2nd generation instrument that combines efforts from MWA and PAPER. 7
HMSFR High-mass Star-forming Region. 116–118, 120, 122, 123, 125, 126
HPC High Performance Computing. 175
HSA High Sensitivity Array. 46, 159, 161

IAA Institute of Applied Astronomy, St. Petersburg, Russia. 11, 100, 168
IAU International Astronomical Union. 131
IceCube IceCube neutrino detector. 146, 147, 153, 180
ICRF International Celestial Reference Frame. 131–134, 152
ICT Information and Communication Technology. 140
IFRS Infra-red Faint Radio Sources. 39
IGM Intergalactic Medium. 89, 93
IGN Instituto Geográfico Nacional, Spain. 11
ILT International LOFAR Telescope. 5, 140
IMBH Intermediate Mass Black Hole. 71, 72, 144
INAF Italian National Institute for Astrophysics. 3
INDIGO Indian Initiative in Gravitational-wave Observations. 144
IPTA International Pulsar Timing Array. 93
IR Infrared light. 35, 36, 38, 43, 44, 85, 86, 107, 113, 121
IRA Istituto di Radioastronomia, Bologna, Italy. 3, 11
ISAS Institute of Space and Astronautical Science. 167
ISM Interstellar Medium. 8, 27, 28, 40, 41, 47, 51, 80, 82, 83, 95, 97, 105, 115, 120
IVIA Iniciativa VLBI IberoAmericana. 140
IVS International VLBI Service. 139, 155, 159, 160

JIVE Joint Institute for VLBI ERIC. 5, 10, 11, 15, 24, 93, 97, 120, 136, 137, 141, 151, 155–157, 169, 170, 174, 175
JPL Jet Propulsion Laboratory. 55, 137, 168
JUMPING Joining up Users for Maximising the Profile, the Innovation and Necessary Globalisation of JIVE. 3, 141
JVAS Jodrell/VLA Astrometric Survey. 21, 23
JVLA Jansky Very Large Array. 15, 37–39, 87, 90, 105, 108, 109, 124, 157, 159, 162
JVN Japanese VLBI Network. 158

KIC Kepler Input Catalog. 97
KIDS KIlo-Degree Survey. 17
KPNO Kitt Peak National Observatory. 147
KVN Korean VLBI Network. 11, 52, 62, 63, 126, 158, 160, 161, 168, 172, 175

LAT *Fermi* Large Area Telescope. 63, 64

LBA LOFAR Low Band Antenna. 163, 164
LBA Long Baseline Array. 15, 52, 107, 139, 160, 161
LC Light-curve. 30
LEAP Large European Array for Pulsars. 95
LIGO Laser Interferometer Gravitational-Wave Observatory. 7, 28, 86, 88, 144
LNA Low-noise Amplifier. 173
LO Local Oscillator. 163
LOCATe LOCalising Astronomical Transients with e-VLBI. 90
LOFAR Low-Frequency Array. 5, 7, 10, 15, 52, 111, 139–141, 149, 163, 164, 175
LSR Local Standard of Rest. 106
LSST Large Synoptic Survey Telescope / Vera C. Rubin Observatory. 7, 17, 79, 142

MALS MeerKAT Absorption Line Survey. 50
mas milliarcsecond. 18, 152
MCP Megamaser Cosmology Project. 27, 29
MeerKAT Karoo Telescope Array. 7, 50, 68, 72, 82, 94, 95, 143, 148, 149, 169, 175
MERLIN Multi-Element Radio Linked Interferometer Network. 21, 22, 25, 39
MPIfR Max Plank Institute for Radio Astronomy, Bonn, Germany. 11, 156
MRO Metsähovi Radio Observatory, Aalto University, Finland. 11
MSP Millisecond Pulsar. 93
MWA Murchison Widefield Array. 164

NAIC National Astronomy and Ionospheric Center. 11
NARIT National Astronomical Research Institute of Thailand. 169
NASA National Aeronautics and Space Administration. 3, 55, 98, 135, 174
NGC New General Catalogue of Nebulae and Clusters of Stars. 28, 40, 46, 48, 52, 68, 86, 116, 117
ngVLA Next Generation Very Large Array. 7, 15, 94, 95, 140, 162, 172
NIRSpec Near-Infrared Spectrograph. 72
NOEMA NOrthern Extended Millimeter Array; formerly Plateau de Bure observatory. 7, 52, 126
NS Neutron Star. 77–80, 88, 93, 94, 147
NVSS NRAO VLA Sky Survey. 165

O3 LIGO/Virgo O3 observing run. 88
OB Early type (O, B) stars. 112, 114, 115
OD Orbit Determination. 135, 136
OH hydroxyl radical. 44, 103, 120, 121, 123, 125, 177
OSO Onsala Space Observatory, Onsala, Sweden. 11

PAF Phased Array Feed. 93, 149
Pan-STARRS1 Panoramic Survey Telescope & Rapid Response System 1. 67
PC Programme Committee. 155, 156
pc parsec. 10
Pierre Auger Observatory Pierre Auger Observatory. 146
PMN Parkes-MIT-NRAO catalog. 24, 25
PMS Pre-main Sequence. 107
PRIDE Planetary Radio Interferometry and Doppler Experiment. 135–137
PTA Pulsar Timing Array. 94

PTF Palomar Transient Factory. 84
PWN Pulsar Wind Nebula. 145

QRFH Quad-Ridge Flared Horn. 172
QTT Qitai 110m Radio Telescope. 159, 169

RAEGE Rede Atlântica de Estações Geodinâmicas e Espaciais. 169
RDBE Roach Digital Backend. 168
RFC Radio Fundamental Catalog. 29
RFI Radio Frequency Interference. 9, 49–52, 89, 90, 92, 93, 96, 97, 165, 168, 171–173, 175
RFSoC Radio Frequency System-on-Chip. 172
RM Rotation Measure. 92, 171
rms root mean square. 21, 26, 42, 46, 71, 94, 113, 114, 125
RSG Red Supergiant. 112

SARAO South African Radio Astronomy Observatory, Cape Town, South Africa. 11, 143
SCORPIO Stellar Continuum Originating from Radio Physics In Our galaxy. 113
SDSS Sloan Digital Sky Survey. 18, 41, 52, 63, 64, 96
SED Spectral Energy Distribution. 38, 64, 88
SETI Search for Extraterrestrial Intelligence. 9, 10, 14, 90, 96, 97
SFG Star-forming Galaxies. 37, 38, 43
SFPR Source Frequency Phase-referencing technique. 62
SFR Star Formation Rate. 38
SFRD Star Formation Rate Density. 35, 36
SFXC Software FX Correlator – EVN software correlator at JIVE. 92, 97, 120, 136, 151, 156, 169, 170, 174
ShAO Shanghai Astronomical Observatory. 11, 168
SHARP Searching for H I Absorption with APERTIF. 49, 50, 52
SiO Silicium Oxide. 103, 117, 120–124, 126, 149
SKA Square Kilometre Array. 5–7, 10, 15, 24, 26, 27, 29, 46, 47, 49–52, 68, 72, 82, 85, 90, 92–95, 105, 111, 126, 127, 134, 140–145, 148–152, 155, 156, 160, 164, 168, 169, 173, 176
SMA Submillimeter Array. 118
SMBH Supermassive Black Hole. 6, 14, 39, 40, 43, 44, 55, 63–71, 73, 75, 84, 85, 147
SMBHB Supermassive Black Hole Binary. 94
SN Supernova. 20, 26, 43, 80–84, 120
SNR Signal-to-Noise Ratio. 62
SpaceX Space Exploration Technologies Corporation. Private American aerospace manufacturer and space transportation services company. 173
SRT Sardinia Radio Telescope. 97, 168
Super-Kamiokande Super-Kamiokande neutrino detector. 147

TAC Time Allocation Committee. 160
TCfA Toruń Centre for Astronomy, Toruń, Poland. 11
TDE Tidal Disruption Event. 84–86, 144
THEZA TeraHertz Exploration and Zooming-in for Astrophysics. 144, 154, 167
TOG Technical and Operations Group. 155, 156
ToO Target of Opportunity. 155, 156

UCD Ultracool Dwarf. 109
UGC Uppsala General Catalogue of Galaxies. 31
uGMRT upgraded Giant Metrewave Radio Telescope. 7, 15, 164, 165
UHECR Ultra-High Energy Cosmic Rays. 146
UHF Ultra High Frequency. 10
ULIRG Ultra-luminous Infrared Galaxies. 38, 42
ULX Ultra-luminous X-ray sources. 40
UT Universal Time. 79
UV Ultraviolet light. 35, 38, 44, 84, 85, 112, 115
UWB-H Ultra Wideband High receiver at Parkes. 161
UWB-L Ultra Wideband Low receiver at Parkes. 161

VDIF VLBI Data Interchange Format. 157, 161, 169, 172, 176
VERA The VLBI Exploration of Radio Astrometry. 123–126, 158
VGOS VLBI Global Observing System. 168
VHE Very High Energy. 145, 146
VIRAC Ventspils International Radio Astronomy Centre, Ventspils, Latvia. 11
Virgo Virgo interferometer, gravitational wave detector. 7, 28, 86, 88, 144
VLA Very Large Array. 7, 22, 37, 39, 44, 52, 71, 78, 80, 81, 88, 113, 114, 118, 124, 126, 162–164
VLASS VLA Sky Survey. 162
VLBA Very Long Baseline Array. 15, 17, 20, 27, 46, 47, 52, 62, 65, 79, 88, 109, 110, 118, 120, 123–126, 139, 145, 156, 159–161, 176
VLBI Very Long Baseline Interferometry. 3, 5–10, 13–15, 17–32, 37–44, 46–52, 55–63, 65–68, 70–72, 77–80, 82–85, 88–98, 103–109, 111, 112, 114–118, 120–127, 131–137, 139–146, 148–152, 154–176
VO Virtual Observatory. 151, 152

WALLABY ASKAP H I All-Sky Survey. 50
WCR Wind Collision Region. 114, 115
WD White Dwarf. 80, 144
WDM Warm Dark Matter. 19, 23
WEAVE next-generation wide-field survey facility for the William Herschel Telescope. 52
Wi-Fi The Standard for Wireless Fidelity. 90
WMAP Wilkinson Microwave Anisotropy Probe. 29
WR Wolf-Rayet type stars. 112, 114, 115
WSRT Westerbork Synthesis Radio Telescope. 7, 41, 93, 147, 168

XAO Xinjiang Astronomical Observatory, Urumqi, China. 11
XRB X-ray Binaries. 40, 57, 77–80

YSO Young Stellar Object. 116–119

ZAMS Zero Age Main Sequence. 118
ZTF Zwicky Transient Facility. 79

The European Space Agency JUICE mission will visit the icy moons of Jupiter. Credit: ESA.